*Journal of the European Ceramic Society* **14** (1994) 493–499

# An Evaluation of Ce–Pr Oxides and Ce–Pr–Nb Oxides Mixed Conductors for Cathodes of Solid Oxide Fuel Cells: Structure, Thermal Expansion and Electrical Conductivity

Marco Nauer,[a] Christos Ftikos[b] & Brian C. H. Steele[a]

[a] Imperial College, Department of Materials, Prince Consort Road, London, UK, SW7 2BP
[b] NTU of Athens, Department of Chemical Engineering, Laboratory of Inorganic Materials Technology, 9 Iroon Polytechniou Str., Athens 15780, Greece

(Received 3 January 1994; accepted 4 May 1994)

***Abstract***

*Ceria doped with praseodymia and niobia has been studied in order to evaluate the possibility of applying these materials as cathodes for solid oxide fuel cells. The content of crystallographic phases and their lattice parameters have been determined by X-ray diffraction, the thermal expansion coefficient has been characterised by the dilatometry technique and the electrical conductivity has been measured by complex impedance spectroscopy and by the four probe DC technique. The results have shown the presence of one fluorite phase in binary compositions ($CeO_2$–$PrO_{2-x}$) for $PrO_{2-x}$ concentrations up to about 20 mol% and two fluorite phases with different lattice parameters for higher $PrO_{2-x}$ concentrations. The addition of 3 mol% $NbO_{2.5}$ has allowed the stabilisation of a single fluorite phase up to 50 mol% $PrO_{2-x}$. The thermal expansion coefficient varies between 0 and 30 × $10^{-6}$/K depending on composition and temperature. The electrical conductivity is mainly electronic and thermally activated. The conductivity exceeds 0·1 S/cm at 800°C for compositions with 40 to 50 mol% $PrO_{2-x}$.*

*Die Arbeit berichtet über die Eignung von $PrO_{2-x}$ und $NbO_{2.5}$-dotiertem $CeO_2$ als Kathoden material für Festkörper–Brennstoffzellen. Die chemische Zusammensetzung der kristallographischen Phasen und deren Gitterparameter wurden durch Röntgenanalyse überprüft und der Wärmeausdehnungskoeffizient durch Dilatometrie bestimmt. Die elektrische Leitfähigkeit wurde mit Hilfe der Impedanzspektroskopie sowie der vierpunkt-DC Technik erhalten. Die Untersuchungen zeigen, daß im Zweistoffsystem ($CeO_2$–$PrO_{2-x}$) mit einem $PrO_{2-x}$-Gehalt bis zu etwa 20 mol% nur eine einheitliche Fluoritphase existiert. Höhere Gehalte an $PrO_{2-x}$ ergeben zwei Fluorit phasen mit deutlich verschiedenen Gitterparametern. Zusätzliche Dotierung mit 3 mol% $NbO_{2.5}$ führt zur Stabilisierung einer einzigen Fluoritphase bis zu 50 mol% $PrO_{2-x}$. Der Wärmeausdehnungskoeffizient (0–30 × $10^{-6}$/K) ändert sich nicht linear mit der Zusammensetzung und der Temperatur. Die Leitfähigkeit ist im wesentlichen elektronisch und thermisch aktiviert. Sie überschreitet 0·1 S/cm bei 800°C für $PrO_{2-x}$-Gehalte zwischen 40 und 50 mol.%.*

*L'oxide de cérium dopé au praseodimium et au niobium a été étudié au fin d'établir la possibilité de son emploi comme cathode de pile à combustible. Le contenu en phases cristallines et leurs paramètres de maille ont été déterminés par diffraction de rayons-X, le coefficient de dilatation a été caractérisé par dilatométrie et la conductivité électrique a été mesurée par spectroscopie d'impédance complexe et par la méthode des quatre points en courant continu. Les résultats ont montré la présence dans le système $CeO_2$–$PrO_{2-x}$ d'une phase fluorite jusqu'à une concentration d'environ 20 mol% de $PrO_{2-x}$ et de deux phases fluorites avec differents paramètres de maille pour des concentrations de $PrO_{2-x}$ plus élevées. L'ajout de 3 mol% de $NbO_{2.5}$ a permis la stabilisation d'une seule phase fluorite jusqu'à 50 mol% de $PrO_{2-x}$. Le coefficient de dilatation thermique n'est pas constant mais varie entre 0 et 30 × $10^{-6}$/K suivant la composition et la température. La conductivité électrique est principalement du type électronique et elle est activée thermiquement. Elle dépasse 0·1 S/cm à 800°C pour les compositions ayant 40 à 50 mol% de $PrO_{2-x}$.*



*Journal of the European Ceramic Society* 0955-2219/94/$7.00 

## 1 Introduction

Cathode materials for solid oxide fuel cells (SOFC) should have the following properties: a high mixed (ionic and electronic) conductivity (0·1 S/cm each), a good chemical stability with the solid electrolyte (yttria-stabilised zirconia), long-term stability in oxidising atmosphere at elevated temperature (1000°C) and a thermal expansion coefficient compatible with that of the solid electrolyte ($10^{-5}$/K for zirconia).

The high ionic conductivity is advantageous in the case of dense cathodes. However, if the ionic conductivity is low, a porous cathode can be applied, as in the case of the presently used perovskite-type La(Sr)–Mn–O based materials. In these materials the maximum oxygen exchange is then achieved through the Faradaic reduction of $O_2$ at the three-phase region.[1] Another perovskite-type material, $La_{0.6}Sr_{0.4}CoO_{3-x}$, shows a sufficiently high ionic conductivity, approximately ten times higher than that of $Zr_{0.9}Y_{0.1}O_{2-x}$ electrolyte material, and therefore could be used as a dense cathode, but unfortunately its high thermal expansion coefficient ($20 \times 10^{-6}$/K) makes it unsuitable for a good bonding to zirconia.[1] Furthermore, these two types of perovskite react with zirconia to form a pyrochlore-type interphase, which is a good ionic conductor in the case of La–Co–O but a poor one in the case of La–Mn–O.

Another class of materials which might be suitable for a cathode is the one based on cerium dioxide. In fact, $CeO_2$ has the same fluorite structure as the stabilised zirconia, a similar thermal expansion coefficient and forms a large solute solubility with zirconia. If $CeO_2$-based materials show sufficiently high electronic and possibly ionic conductivities, then they might replace La–Mn–O perovskite for future SOFC.

Unlike the case of perovskite oxides, which are metallic-like conductors, the electronic conduction in $CeO_{2-x}$ occurs through the motion of small polarons by a thermally activated hopping mechanism (diffusion-like motion).[2,3] The hopping involves an electron jumping from the $Ce^{3+}$ to a neighbouring $Ce^{4+}$ ion, and the maximal electronic conductivity is expected for a $Ce^{3+}/Ce^{4+}$ ratio equal to 1. In pure ceria, $Ce^{3+}$ ions are formed at high temperature and in reducing atmosphere, while in oxidising atmosphere $Ce^{3+}$ ions can be introduced by substituting a tetravalent cerium ion with a pentavalent ion (e.g. $Nb^{5+}$),[4] thus reducing $Ce^{4+}$ to $Ce^{3+}$ in order to maintain charge neutrality. Under high pressure (>1 atm) oxygen interstitials as compensating defects are formed.[4]

In order to increase the ionic conductivity, oxygen vacancies in the material need to be created. An amount of approximately 2·5% oxygen vacancies has often been found to be ideal for achieving the maximum ionic conductivity in related $ZrO_2$ fluorite materials.[5] This can be achieved in ceria by doping $CeO_2$ with a di- or trivalent element.

Praseodymium is known to have a mixed valence (III, IV) in $PrO_{2-x}$ at atmospheric pressure, the molecular formula being $PrO_{1.833}$ at room temperature and $PrO_{1.77}$ at 800°C.[6] As for cerium dioxide, electron hopping mechanisms occur between $Pr^{3+}$ and $Pr^{4+}$ ions.[7,8] In the fluorite phase of $PrO_{2-x}$ paired oxygen vacancies create a short-range order along ⟨111⟩ directions and praseodymium ions with various coordination numbers (Vl, VII, VIII). The magnitude of electrical conductivity is mainly due to the concentration of Pr(VII).[8] It is therefore possible, through the addition of $PrO_{2-x}$ to $CeO_2$, to introduce oxygen vacancies in the fluorite structure in order to increase the ionic conductivity and $Pr^{3+}$, $Pr^{4+}$ ions in order to increase the electronic conductivity. Indeed, Takasu *et al.*[9] showed that Ce–Pr–O solid solutions are mixed conductors. From their results it appears that $Ce_{0.6}Pr_{0.4}O_{2-x}$ shows the best ionic and electronic conductivities in this system. By extrapolating their data to 800°C, a promising total conductivity of 0·15 S/cm is obtained.

The aim of this work is therefore to further investigate the Ce–Pr oxide system, also with the addition of niobium, and to evaluate the possibility of applying these materials as cathodes for solid oxide fuel cells. The structure and lattice parameters of the formed phases, the thermal expansion and the electrical conductivity of Ce–Pr oxides and Ce–Pr–Nb oxides will be presented.

## 2 Materials Preparation and Experimental Procedures

The oxide powders were prepared by a coprecipitation process following the method used by Groot Zevert *et al.*[10] for yttria-doped zirconia. As starting precursors 99·9% $Pr_6O_{11}$, 99·99% $Ce(NO_3)_36H_2O$ and 99·9% $NbCl_5$ were used. $Pr_6O_{11}$ was dissolved in concentrated $HNO_3$, $Ce(NO_3)_36H_2O$ in water and $NbCl_5$ in concentrated HCl. The mixed solution (0·2 M) was added slowly to a $NH_3$/water solution (pH ≥ 13) and the coprecipitated gel was washed five times in $NH_3$/water solutions with decreasing $NH_3$ concentration and three times in absolute (99·7%) ethanol. The dried (120°C, air) hydroxide gel was ground, milled in ethanol and calcined for 2 h at 800°C. The oxide powder was milled again for 2 h in ethanol with 1 wt% PVB binder. Compositions of the prepared powders are shown in Table 1. The particle size analysis of the powders shows a

**Table 1.** Composition of materials studied

| *Composition* |
|---|
| $Ce_{0.80}Pr_{0.20}O_{2-x}$ |
| $Ce_{0.60}Pr_{0.40}O_{2-x}$ |
| $Ce_{0.50}Pr_{0.50}O_{2-x}$ |
| $Ce_{0.77}Pr_{0.20}Nb_{0.03}O_{2-x}$ |
| $Ce_{0.57}Pr_{0.40}Nb_{0.03}O_{2-x}$ |
| $Ce_{0.47}Pr_{0.50}Nb_{0.03}O_{2-x}$ |

narrow distribution with a mean particle diameter of 0·8 $\mu$m and X-ray analysis shows a single fluorite phase for all the compositions.

Pellets and bars were prepared by uniaxial compacting under low stress (30 MPa) followed by isostatic pressing under 170 MPa. This procedure has been proved to be effective in avoiding cracking during sintering which often occurred in purely uniaxially compressed samples, probably as a consequence of inhomogeneous green density. Samples were sintered in air at 1550°C for 10 h. Final densities, measured by the Archimedes' method in water, are 94–98% of theoretical, where higher densities are obtained for compositions with lower praseodymium content. The grain size of the samples is about 10 and 8 $\mu$m for compositions with and without niobium, respectively. A typical microstructure of these materials is shown in Fig. 1.

The phase content of sintered materials and their lattice parameter were measured by X-ray diffraction on a Philips PW 1710 Diffractometer operated at 40 kV and 40 mA ($CuK_\alpha$). XRD spectra were obtained by scanning continuously at a rate of 1°2$\theta$/min with a slit angle of 1° and using silicon as external calibration. The lattice parameters were calculated by using a least squares refinement program.

The total electric conductivity has been measured by the four probe DC method on bars and pellets (two electrodes on each side of the pellet) and by AC impedance spectroscopy (0·1 Hz–10 MHz) on pellets. The latter has been performed using a Schlumberger Solartron 1260 impedance analyser controlled by a microcomputer.

Finally, the thermal expansion coefficient has been measured with a dilatometer between 200 and 1400°C in air.

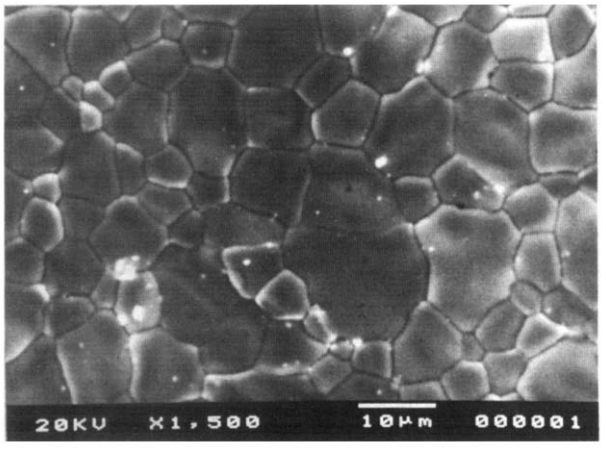


**Fig. 1.** Typical microstructure of Ce–Pr oxides and Ce–Pr–Nb oxides sintered for 10 h at 1580°C, illustrated by $Ce_{0.47}Pr_{0.50}Nb_{0.03}O_{2-x}$.

## 3 Results and Discussion

### 3.1 Phase analysis and lattice parameters

Lattice parameters obtained by X-ray diffraction of sintered pellets (1550°C/10 h) are shown in Fig. 2(a) and (b). Cerium–praseodymium oxide shows the presence of a single phase with the cubic fluorite structure up to a $PrO_{2-x}$ content of 30 mol%, followed by a domain with two fluorite phases at least up to 60 mol% $PrO_{2-x}$. The lattice parameter of the fluorite phase close to the $CeO_2$ boundary slightly decreases with increasing

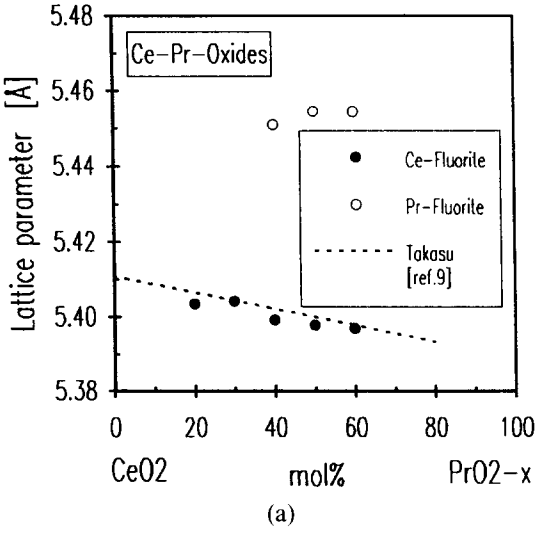


(a)

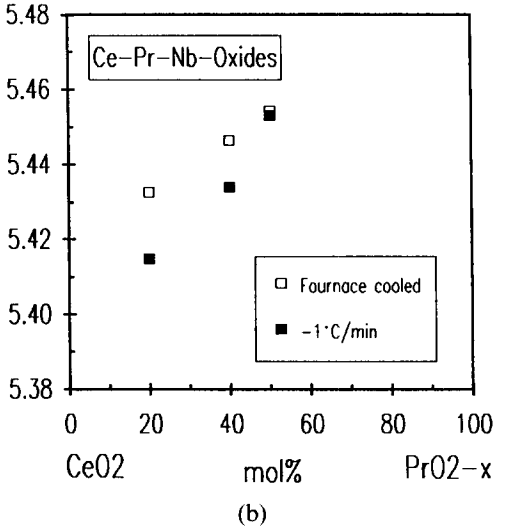


(b)

**Fig. 2.** Lattice parameters of fluorite phases in (a) Ce–Pr oxides and (b) Ce–Pr–Nb oxides.

praseodymium content, while the lattice of the second phase, richer in praseodymium, is close to 5·455 Å. These results disagree with those reported by Takasu *et al.*,[9] which showed the presence of a single fluorite phase up to 70 mol% $Pr_6O_{11}$ in materials sintered for 50 h at 1400°C. The same sintering cycle has been applied to the present materials in order to exclude any possible influence of sintering conditions, but no changes in the results were observed. Another possible influence might arise from the applied cooling rate, because praseodymium is expected to decrease the $Pr^{3+}/Pr^{4+}$ ratio during cooling by absorbing oxygen and equilibrium might not be attained due to slow oxygen diffusion at low temperature.

The amount of the two fluorite phases of the binary system, named Ce-Fluorite ($CeO_2$-rich) and Pr-Fluorite ($PrO_{2-x}$-rich) has been derived from XRD spectra assuming that the relative fraction of the two phases is equal to relative intensities of their peaks. Surprisingly, the amount of the second phase, rich in praseodymium, increases from 35% for the material with 40 mol% $PrO_{2-x}$ to 83% for 50 mol% $PrO_{2-x}$ and then decreases again to 8% for 60 mol% $PrO_{2-x}$. These results do not allow calculation of the boundary between the compositions with one and two fluorite phases. This problem and the discrepancy between the present results and those obtained by Takasu *et al.*,[9] require further investigations in order to be clarified.

Niobium oxide has a low solubility limit, 0·6 mol% $Nb_2O_5$, in pure ceria,[4] but work done by Liddicot & Steele (pers. commun.) on $CeO_2$–$Y_2O_3$–$Nb_2O_5$ solid solutions showed that the solubility limit of niobium oxide in ceria solid solutions can be increased if the excess oxygen of $Nb_2O_5$ is compensated by oxygen vacancies introduced by a low-valent doping element. In the case of ceria doped with praseodymia, assuming that the concentration of trivalent and tetravalent Pr ions are approximately equal, 3 mol% $NbO_{2.5}$ should be completely soluble starting from a $PrO_{2-x}$ content of 3 mol%, i.e. from concentrations much lower than those applied in this work. In fact, the addition of 3 mol% $NbO_{2.5}$ did not lead to second phases related to the doping with niobium and furthermore it allowed the stabilisation of a single fluorite phase up to at least 50 mol% $PrO_{2-x}$. The most remarkable effect obtained from the addition of a small amount of niobium appears to be its tremendous influence on the lattice parameter of $CeO_2$–$PrO_{2-x}$–0·03$NbO_{2.5}$ solid solutions, as shown by the comparison of Fig. 2(a) and (b). Since the low doping level of $Nb_2O_5$ hardly influences the concentration of oxygen vacancies by the addition of its extra oxygen, this effect must arise by the presence of $Nb^{5+}$ itself, e.g. by its influence on the oxidation state of praseodymium and/or cerium ions or by a different arrangement of point defects/complexes.

A comparison between materials cooled down by turning off the furnace (the standard procedure) and cooled down with a rate of −1°C/min did not show any influence of the cooling rate on the structure but variations in the lattice parameters were observed (Fig. 2(b)). The lattice parameter decreases when samples were cooled down slowly (−1°C/min) from the sintering temperature, i.e. by allowing the attainment of a state closer to equilibrium. This is believed to arise from a lower $Pr^{3+}$ concentration and a higher oxygen content in the material. The difference of lattice parameters is particularly pronounced in samples with 20 and 40 mol% $PrO_{2-x}$. Variations of the oxygen partial pressure during sintering would also affect the $Pr^{3+}/Pr^{4+}$ ratio, but in the present work all the experiments were carried out in air.

### 3.2 Thermal expansion coefficient

Thermal expansion experiments were performed on materials containing a single fluorite phase. The results reported in Fig. 3 show that all the compositions have a highly non-linear thermal expansion in the temperature range 200 to 1400°C. For all the compositions the thermal expansion coefficient $\eta$ is 12·5–13$\times 10^{-6}$/K for temperatures lower than 300°C. The materials with 20 mol% $PrO_{2-x}$ show a strong decrease of $\eta$ in the temperature range 400 to 700°C ($Ce_{0.80}Pr_{0.20}O_{2-x}$) and 400 to 600°C ($Ce_{0.77}Pr_{0.20}Nb_{0.03}O_{2-x}$). The addition of niobium in $Ce_{0.77}Pr_{0.20}Nb_{0.03}O_{2-x}$ causes a sharper and stronger decrease of the thermal expansion coefficient, which in fact reaches a negative minimum ($-1{\cdot}6\times 10^{-6}$/K) at 500°C. On the other hand, doping with niobium decreases the maximum of thermal expansion coefficient observed at 800°C,

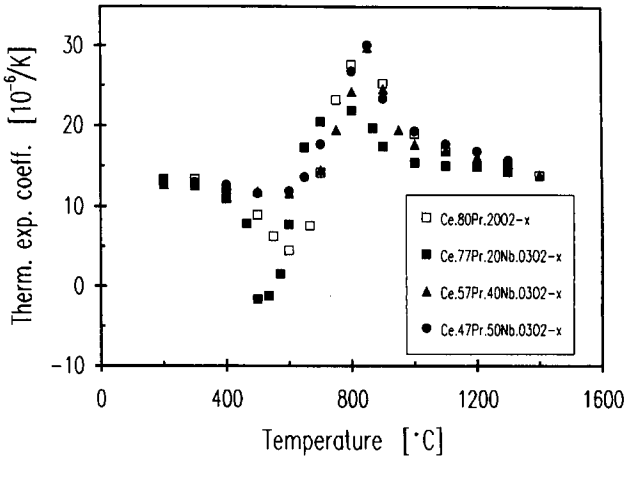


**Fig. 3.** Thermal expansion coefficient of Ce–Pr oxides and Ce–Pr–Nb oxides (heating rate: 5°C/min).

$21{\cdot}9\times10^{-6}$/K for $Ce_{0.77}Pr_{0.20}Nb_{0.03}O_{2-x}$ compared to $27{\cdot}6\times10^{-6}$/K for $Ce_{0.80}Pr_{0.20}O_{2-x}$. For both compositions the thermal expansion coefficient reaches a constant value of $15\times10^{-6}$/K at higher temperatures, i.e. higher than 1000°C for $Ce_{0.77}Pr_{0.20}Nb_{0.03}O_{2-x}$ and higher than 1200°C for $Ce_{0.80}Pr_{0.20}O_{2-x}$. The thermal expansion coefficient of the compositions with higher praseodymium content, 40 and 50 mol% $PrO_{2-x}$ for $Ce_{0.57}Pr_{0.40}Nb_{0.03}O_{2-x}$ and $Ce_{0.47}Pr_{0.50}Nb_{0.03}O_{2-x}$, respectively, is fairly constant up to 600°C but then increases strongly and reaches a maximum value of $30\times10^{-6}$/K at 800°C. The thermal expansion coefficient again reaches the same value as for the composition with lower praseodymium content at high temperatures, i.e. $16\text{–}14\times10^{-6}$/K at 1200–1400°C.

The strong increase of the thermal expansion coefficient in the temperature range 600 to 1000°C is believed to arise from the loss of oxygen and the associated reduction of $Pr^{4+}$ to $Pr^{3+}$, a change of valence which causes an increase of the ionic radius (1·27 Å for $Pr^{3+}$ compared to 1·10 Å for $Pr^{4+}$ for eight-fold coordination[11]). The occurrence of a decrease in thermal expansion for the composition with 20 mol% $PrO_{2-x}$ in the temperature range 400 to 600°C has not been clarified at present.

The thermal expansion behaviour observed for Ce–Pr oxides and Ce–Pr–Nb oxides could compromise their use as cathode materials for solid oxide fuel cells.

### 3.3 Electrical conductiviy

Two typical impedance spectra of the material investigated are shown in Fig. 4. The two curves represent the spectra of $Ce_{0.77}Pr_{0.20}Nb_{0.03}O_{2-x}$ and $Ce_{0.57}Pr_{0.40}Nb_{0.03}O_{2-x}$ obtained at room temperature. A behaviour similar to that of $Ce_{0.77}Pr_{0.20}Nb_{0.03}O_{2-x}$ has also been observed for the other material containing 20 mol% $PrO_{2-x}$, $Ce_{0.80}Pr_{0.20}O_{2-x}$, while the behaviour of $Ce_{0.57}Pr_{0.40}Nb_{0.03}O_{2-x}$, i.e. only one semicircle, has been observed in all the other

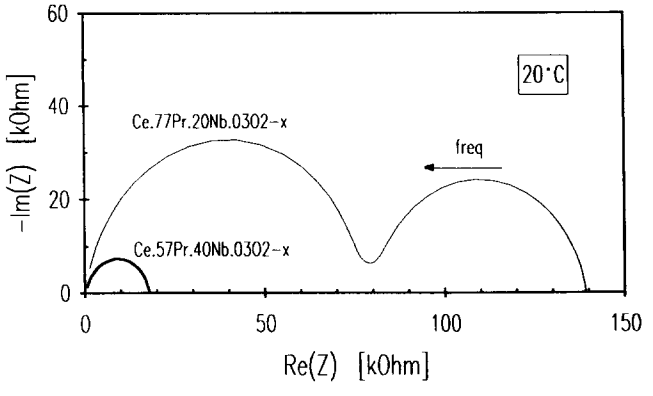


**Fig. 4.** Typical impedance spectra at room temperature of Ce–Pr oxides and Ce–Pr–Nb oxides (frequency range in this figure: $1\text{–}10^6$ Hz).

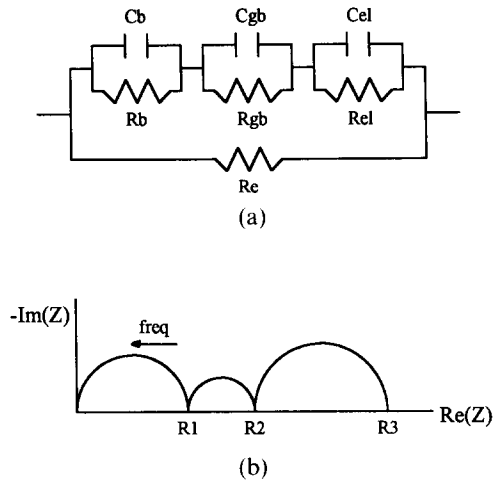


**Fig. 5.** Equivalent circuit for mixed conductivity (a) and corresponding impedance plot (b). $R1 = [1/R_e + 1/R_b]^{-1}$, $R2 = [1/R_e + 1/(R_b + R_{gb})]^{-1}$, $R3 = [1/R_e + 1/(R_b + R_{gb} + R_{el})]^{-1}$.

materials containing 40 and 50 mol% $PrO_{2-x}$ ($Ce_{0.60}Pr_{0.40}O_{2-x}$, $Ce_{0.50}Pr_{0.50}O_{2-x}$, $Ce_{0.47}Pr_{0.50}Nb_{0.03}O_{2-x}$). The spectra have been analysed by assuming the equivalent circuit model shown in Fig. 5(a). The total impedance is given by the parallel contribution of ionic and electronic impedances, where the ionic one is expressed as usual by a series of combined elements (resistance $R$ with a parallel capacitance $C$) representing the bulk (b), grain boundary (gb) and electrode (el) polarisations, while the electronic impedance is represented by a pure resistive element $R_e$. The frequency response of such a circuit is shown in the Cole–Cole plot of Fig. 5(b). A simulated spectrum is fitted to a measured one by the method of the least squares in order to estimate the value of the elements of the circuit shown in Fig. 5(a). An example of a fitted spectrum is given in Fig. 6 for the material $Ce_{0.77}Pr_{0.20}Nb_{0.03}O_{2-x}$ tested at 21°C between 1 and $10^{-6}$ Hz. The simulated spectrum gives a good estimation of the real and imaginary part of the impedance. From the model presented in Fig. 5 it could be clarified that two semicircles appear

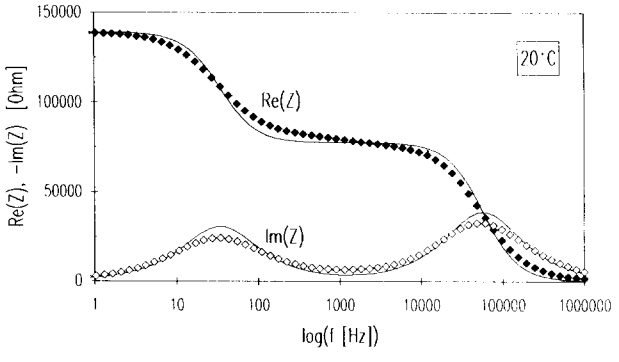


**Fig. 6.** Comparison between measured and simulated impedance spectra of material $Ce_{0.77}Pr_{0.20}Nb_{0.03}O_{2-x}$. $R_b = 1{\cdot}55\times10^5\ \Omega$, $C_b = 36$ pF, $R_{gb} = 1{\cdot}20\times10^6\ \Omega$, $C_{gb} = 19$ nF, $R_e = 1{\cdot}55\times10^5\ \Omega$ ($R_{el} = 10^8\ \Omega$, $C_{el} = 10\ \mu$F).

only when the ionic contribution to the total conductivity is appreciable while one semicircle appears when the electronic conductivity is much larger than the ionic one (ionic transference number $t_i < 0{\cdot}01$). The systematic absence of the third semicircle implies that the resistance due to the electrode reaction is much larger than the electronic resistance.

The different contributions to the total conductivity of the different materials could be estimated for materials with more than one semicircle, i.e. $Ce_{0{\cdot}80}Pr_{0{\cdot}20}O_{2-x}$ and $Ce_{0{\cdot}77}Pr_{0{\cdot}20}Nb_{0{\cdot}03}O_{2-x}$. The ionic bulk ($\sigma_b$) and grain boundary ($\sigma_{gb}$) conductivities and the electronic conductivity ($\sigma_e$) at room temperature were calculated to be $3{\cdot}9\times10^{-7}$, $2{\cdot}5\times10^{-8}$, $1{\cdot}1\times10^{-6}$ S/cm for $Ce_{0{\cdot}80}Pr_{0{\cdot}20}O_{2-x}$ and $8{\cdot}4\times10^{-7}$, $1{\cdot}1\times10^{-7}$, $8{\cdot}4\times10^{-7}$ S/cm for $Ce_{0{\cdot}77}Pr_{0{\cdot}20}\cdot Nb_{0{\cdot}03}O_{2-x}$. It can be noticed that the ionic transference numbers at room temperature are 0·02 and 0·11 when grain boundary resistivity are included. For the other materials the ionic transference number is smaller than 0·01. From the analysis of the spectra it follows that the total conductivity measured corresponds fairly well to the electronic one when only one semicircle appears in the Cole–Cole plot, i.e. for $PrO_{2-x}$ fractions equal 0·4 and 0·5, while for materials which show two semicircles, i.e. $Ce_{0{\cdot}80}Pr_{0{\cdot}20}O_{2-x}$ and $Ce_{0{\cdot}77}Pr_{0{\cdot}20}\cdot Nb_{0{\cdot}03}O_{2-x}$, the total conductivity equals $[1/R_e + 1/(R_b + R_{gb})]$. In the latter case the electronic and ionic contributions should be separated in order to analyse the evolution of conductivity with temperature but the semicircle at high frequencies collapses at higher temperature as a consequence of a decreasing time constant and increasing relative noise of the impedance analyser, making the spectrum unsuitable for analysis. Consequently, in the following, apparent activation energies will be determined from the measured total conductivities.

The total electrical conductivity of different materials measured on pellets and on bars are shown in Fig. 7(a) and (b) as a function of the reciprocal of the absolute temperature. The conductivity data obtained on pellets are generally 2–3 times higher than those obtained on bars at low temperatures, while the contrary is true at high temperatures. Since bars and pellets have been prepared from the same powders and sintering cycle such differences remain unexplained at present. Electrical conductivities reported in Fig. 7 are significantly higher than those reported by Takasu *et al.*[9] for the same praseodymium concentration. The addition of 3 mol% $NbO_{2{\cdot}5}$ does not lead to major differences in the electrical conductivities, with the exception of materials with 50 mol% $PrO_{2-x}$ in which the disagreement may arise from the different phases present in

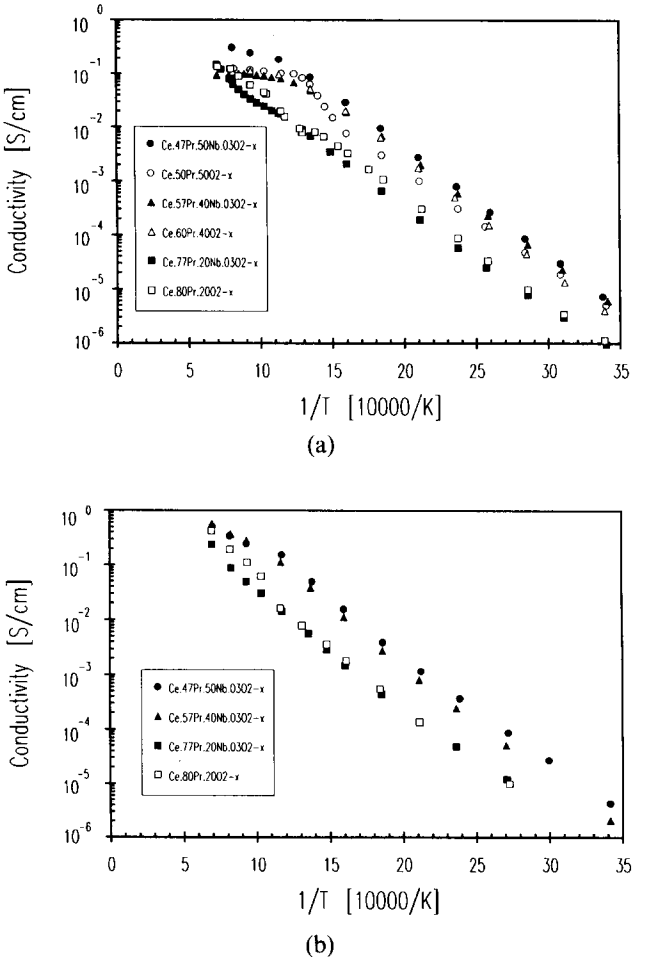


**Fig. 7.** Total electrical conductivity versus $1/T$ of Ce–Pr oxides and Ce–Pr–Nb oxides measured by the four-points technique on (a) pellets and (b) bars.

the two materials (see Section 3.1). The highest electrical conductivities are obtained for materials with 40 and 50 mol% $PrO_{2-x}$ and are well above 0·1 S/cm at 800°C.

The conducting mechanism(s) appears to be thermally activated but the log ($\sigma$) versus $1/T$ curves do not follow a straight line over the entire temperature range. They generally show a slight increase in the slope between 200 and 250°C and also more evident discontinuities at higher temperatures, indicating that either more than one conducting mechanism is involved and/or that the number of charge carriers varies with temperature. The latter assumption has already been suggested by results obtained on thermal expansion.

Assuming that electronic conductivity is dominant and that the charge carriers are small polarons, activation energies have been calculated following the relationship

$$\sigma T^{3/2} = \sigma_0 \exp\left[-E_a/k_B T\right] \qquad (1)$$

where $\sigma$ is the conductivity, $E_a$ the apparent activation energy, $\sigma_0$ a preexponential factor, $k_B$ is the Boltzmann constant and $T$ the absolute temperature. Equation (1) follows from

$$\sigma = n\mu e$$

where $n$ is the carrier concentration, $e$ their charge and $\mu$ their mobility, and the relationship between small polarons mobility and temperature,[12]

$$\mu = \mu_0 T^{3/2} \exp[-E_h/RT]$$

where $E_h$ is the activation energy for hopping and $\mu_0$ a constant. The apparent activation energy $E_a$ differs from $E_h$ if the concentration of carriers varies with temperature. This is indeed true in the present case, although the two values should not differ significantly because the variation in carrier concentration is much smaller than one order of magnitude. Furthermore, the equation $\sigma = n\mu e$ is valid for dilute solutions, while in the present case interactions between point defects may occur. In fact, although electrical conductivity increases with increasing praseodymium content, proportionality between $\sigma$ and $n$ is not respected (it is assumed that $n$ is proportional to praseodymium content, although cerium may also contribute to conductivity, in particular at temperatures higher than 500°C).

Apparent activation energies have been calculated only for materials containing a single phase on measurements obtained by the four-probe DC technique on bars (Fig. 7(b)). Their values are the same for all the compositions and vary from 0·42 ± 0·02 eV for $T$ < 200°C to 0·53 ± 0·02 eV for 200°C < $T$ < 600°C. Above 600°C the log $\sigma$ versus $1/T$ curves are not linear and therefore activation energies have not been calculated. Nevertheless it can be noticed that materials with high praseodymium content (40 and 50 mol% $PrO_{2-x}$) show a low temperature dependency while materials containing 20 mol% $PrO_{2-x}$ show an increasing apparent activation energy. The activation energies below 600°C are quite low and in agreement with a small polaron hopping mechanism. In pure non-stoichiometric $CeO_{2-x}$ activation energies for small polaron hopping were found to be 0·2–0·5 eV, depending on the defect concentration.[2,4]

The broad quasi-flat maximum of electrical conductivity observed at high temperatures (Fig. 7(a) and (b)) is similar to that observed in $CeO_{2-x}$. Tuller & Nowick[2] attributed it to short-range order present at high values of $x$ (0·1) which would immobilise some of the carriers.

## 4 Summary and Conclusions

$PrO_{2-x}$ is soluble in ceria up to a concentration of approximately 30 mol%, while for higher concentrations a second fluorite phase with a bigger lattice parameter is formed. The addition of 3 mol% $NbO_{2.5}$ stabilises a single fluorite phase up to at least 50 mol% $PrO_{2-x}$.

The thermal expansion of Ce–Pr oxides and Ce–Pr–Nb oxides is highly non-linear. The thermal expansion coefficient varies from about 0 to $30 \times 10^{-6}$/K depending on temperature and composition. In general, the thermal expansion coefficient is $12{\cdot}5–13 \times 10^{-6}$/K up to 400°C, shows a minimum value between 500 and 600°C and a maximum value at 800°C, and again becomes constant above 1000–1200°C ($\sim 1{\cdot}5 \times 10^{-6}$/K).

Electrical conductivity in Ce–Pr oxides and Ce–Pr–Nb oxides is thermally activated and the main contribution to conductivity is given by electrons. The electrical conductivity increases with increasing praseodymium content and values higher than 0·1 S/cm at 800°C are obtained.

## Acknowledgements

The contribution of R. Rudkin for technical assistance is gratefully acknowledged. One of the authors (M. Nauer) would also like to thank the Swiss National Science Foundation for its financial support.

## References

1. Steele, B. C. H., Carter, S., Kajda, J., Kontoulis, I. & Kilner, J. A., In *Proceedings of the Second International Symposium on Solid Oxide Fuel Cells*, ed. F. Grosz & P. Zegers. CEC Publication EUR 13546 EN, Luxembourg, 1991, p. 517.
2. Tuller, H. L. & Nowick, A. S., *J. Phys. Chem. Solids*, **38** (1977) 859.
3. Naik, I. K. & Tien, T. Y., *J. Phys. Chem. Solids*, **39** (1978) 311.
4. Naik, I. K. & Tien, T. Y., *J. Electrochem. Soc.*, **126** (1979) 562.
5. Nakamura, A. & Wagner Jr., J. B., *J. Electrochem. Soc.*, **133** (1986) 1542.
6. Hyde, B. G., Bevan, D. J. M. & Eyring, L., *Phil. Trans. Royal Soc. London Scr. A*, **259** (1966) 583.
7. Honig, J. M., Cella, A. A. & Cornwell, J. C., *Rare Earth Res.*, **2** (1964) 55.
8. Inaba, H. & Naito, K., *J. Solid State Chem.*, **50** (1983) 100, 111.
9. Takasu, Y., Sugino, T. & Matsuda, Y., *J. Appl. Electrochem.*, **14** (1984) 79.
10. Groot Zevert, W. F. M., Winnubst, A. J. A., Theunissen, G. S. A. M. & Burggraaff, A. J., *J. Mater. Sci.*, **25** (1990) 3449.
11. Shannon, R. D., *Acta Cryst.*, **A32** (1976) 751.
12. Friedman, L. & Holstein, T., *Ann. Phys.*, **21** (1963) 494.